Investigating a Total Hip Arthroplasty Finite Element Model with Respect to the Offset and Version Changes, According to the Modular Neck Type

E. G. Theodorou[1], C. G. Provatidis[2,*], P. D. Megas, MD[3]

[1,2] National Technical University of Athens, School of Mechanical Engineering, Mechanical Design & Control Systems   Section, Laboratory of Dynamics and Structures
NTUA Campus, Zografou, 9 Heroes of Politechnion, GR-15780 Athens, Greece
[1] etheod@mail.ntua.gr, etheod@gmail.com, [2] cprovat@central.ntua.gr
[3] Orthopaedics Department, Medical School, University of Patras,
Rio, 26504, Greece
panmegas@med.upatras.gr
* National Technical University of Athens
School of Mechanical Engineering
Mechanical Design and Control Systems Section, Biomechanics Unit

Prof. Dr.-Ing. Christopher G. Provatidis

9, Heroes of Polytechnion Avenue, Zografou Campus
GR-157 80 Athens, Greece
Tel: +30-210-772.1520   Fax: +30-210-772.2347
E-mail: cprovat@central.ntua.gr
URL: http://users.ntua.gr/cprovat

Abstract

Over the past years total hip arthroplasty has become the golden standard as far as the reconstruction of the hip joint is concerned. The younger and more active patients are increasing constantly and the use of *modular* implant systems is considered as one of the best available options since they provide extensive flexibility and revision possibilities. Many parameters affect the longevity and the stability of the implants but in the current study we focus on the effects of neck modularity in the overall biomechanical behavior of the bone and its femoral components. The acquisition of a Computed Tomography scan set from a cadaveric femur and the implementation of a *Profemur-E* system with six modular necks: straight, 8° retroversion and 15° anterversion (*short & long*) along with a typical femoral head, resulted in the development of a full scale three dimensional finite element model. Under a one-legged stance phase loading scenario, the numerical results revealed significant alterations in stresses and strains in the bone implant assembly. The neck pair positioned with retroversion produced significantly higher values, especially for neck stress and bone strains. The Ti Alloy stem had also higher stress concentrations for the long retroverted neck. The equivalent von Mises strains of the femur were examined with respect to Frost's Law for bone growth activity. It was shown that all six models, although variations both numerically and visually existed in their distributions, had similar behavior. For the region of the lesser trochanter the use of short neck invoked lower strains with possible bone loss. Finally, two profile lines were isolated, enclosing the greater and lesser trochanter, and their corresponding node values were plotted respectively, with the short and long retroverted necks being in the upper regions of the chart. Peak (lateral

side) – and some local minimum values (medial side) – of the outer cortical bone were located at the stem tip zone, in accordance with the applied load for a properly positioned stem.

Keywords: total hip arthroplasty, finite elements, modular implants, profemur-e, Ansys

1. Introduction

In the vital area of Orthopedic Biomechanics, it is undisputed that Total Hip Arthroplasty has become a major research field. Several pathological cases in the hip region, such as osteoarthritis, femoral head necrosis (Brinker et al. 1994; Min et al. 2008) are currently treated with the specific surgical operation, in which the acetabulum socket and the upper part of the femur – ball-and-socket joint (Sariali et al. 2008) – are removed and replaced by a hip implant system.

Starting off with the original designs by Sir John Charnely (Charnley 1972) and the first attempts to fully restore one of the major joints of the human body, significant progress has been made in the development of new, improved and more advanced hip implant systems, in order to cope with the more active way of life of much younger patients.

Focusing our interest mainly on the femoral components the main designs consist of a monolithic implant with three major areas: the main body – providing proximal and distal fixation, the neck and finally the head that will cooperate with the corresponding implant on the pelvis. Aiming to find a more stable and versatile implant solution, modular hip implant systems have been introduced (Werner et al. 2000; Bono 2001). Currently the orientation of these systems aims on the hip anatomy in order to achieve the best possible fit in the femur of the patient and restore the soft tissues to their previous tension, position and morphology (Sariali et al. 2008). This led to the creation of a wide range of products covering several anatomical alterations and clinical symptoms.

In more details, when undergoing a THA operation, the desired result is the restoration of the joint functionality by correcting leg length and offset and minimizing the risk of complications such as dislocation and limp (Dostal et al. 1981). These two main factors are easily satisfied by the use of modular implant systems. Depending on the retail product at hand, a range of different necks and femoral heads is available and their combination leads to variable joint centers and restoration options. During the preoperative planning the orthopaedist calculates the correct new position of the femur and during surgery some fine adjustment are performed with the use of trial necks and heads leading to optimized fixation, best range of motion and limb length (Dostal et al. 1981; Sariali et al. 2008, Sariali et al. 2009). Minor adjustments and improvements of the original preoperative plan can also be performed during the surgical operation and compensate for difficulties that may arise.

Although the mechanical properties of modular implants are thoroughly examined before going into production, their biomechanical behavior remains under investigation. Recent studies focus mainly on clinical failure (Chu et al. 2001; Sporer et al. 2006) and only few on the influence of modularity on stresses and strains developed on areas of clinical interest.

Towards this direction the current study aims – using Computer Tomography (CT) data for identifying the bone anatomy and combining it with modern Computer Aided Design (CAD) software and computational mechanics, namely Finite Element Analysis (FEA) – to isolate and investigate the effect that modular neck length may impose on the strains and stresses of the bone implant assembly.

2. Materials and methods

For the investigation of the behavior of a Total Hip Arthroplasty using a modular hip system under different neck lengths (offset values), the Finite Element Method was chosen: a model was generated based on CT data for the femur and loading scenarios, as found in literature, were applied.

2.1 Cadaveric Femur

For the creation of the three dimensional model, although current studies (Completo et al. 2007, Rietbergen et al. 1993) use about one third of the femur length, it was decided to scan and digitize the full bone geometry. Using a Siemens Senasation 4 CT Scanner and with slice thickness set to one millimeter, a DICOM archive of a cadaveric - 35 year old - femur (Fig. 1b) was obtained.

The first step of the preprocessing was performed with the use of MIMICS v.8 (Materialise NV), as shown in Figure 1a. The CT scans were individually processed, providing the full femur geometry as a point could. Using Geomagic Studio v.9 (Geomagic, Inc.), the points were then converted into the bone volume (Fig. 1c) and the resulting three dimensional CAD Model – *step file* – was imported into Solidworks 2008 – 2009 (Dassault Systèmes SolidWorks Corp.) for further steps (Fig. 1d).
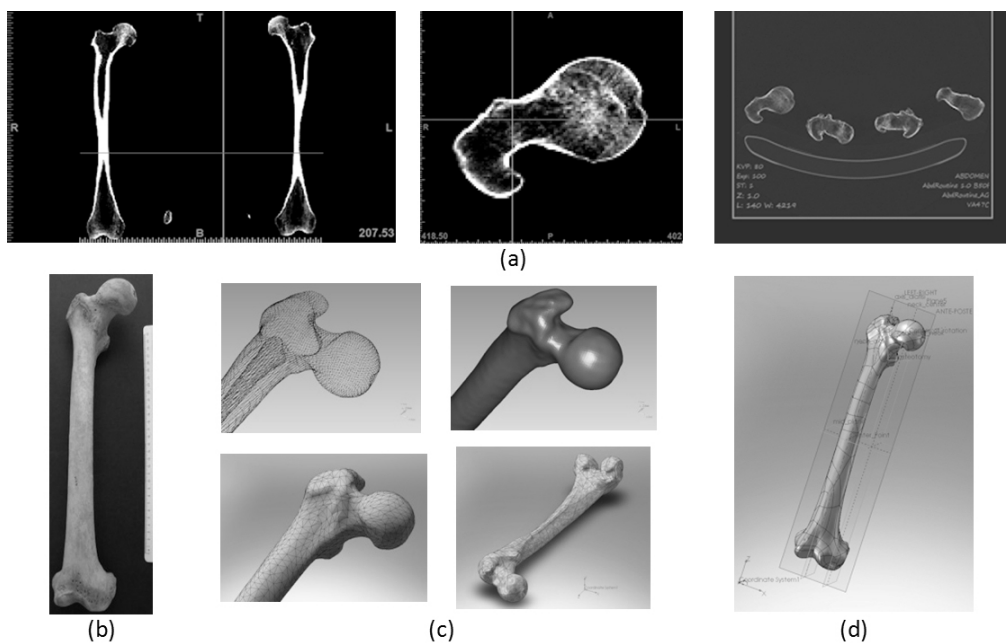

Figure 1. From Cadaveric Femur to CAD model: a) Step by step image processing of the CT scans using Mimics, b) Cadaveric Femur, c) Converting the derived point could to a 3D solid model, d) Digital Pre-operative Templating and dimensioning.

With the 3D CAD-model fully processed, the preoperative planning is the next step. Using the anteroposterior X-Ray, the CT scans and the implant's templates, a very good estimate for the proper stem size and the necessary neck and head was established. All the basic geometrical reference elements (diaphyseal axis, neck axis, Center of Rotation) were found on the 3D model

with the assistance of a set of control points, axis and curves (Della Valle et al. 2005). All required measurements were then integrated into the model and recorded (Fig. 1d). With the aforementioned elements, the modular implant system was chosen.

2.2 Profemur-E Modular Hip Implant

Keeping in mind that the modularity was the main criterion for the selection of the implant system, the study was based upon the Profemur-E hip system, by Wright® Medical Technologies, since the combination of the twelve necks with the available femoral heads can lead up to more than hundred different positions (Fig. 2a). Currently three neck sets are under investigation namely the straight (long & short), an 8° retroverted (long & short) and a 15° anteverted (long & short) along with a 28 mm normal (*no additional offset*) femoral head. In order to digitize the implants, a Coordinate Measurement Machine (CMM), Mistral 07075 by DEA–Brown & Sharpe Inc. with a Renishaw PH10M scanning head with compliance to ISO 10360–2 standard, was used.

Figure 2b shows a Number 5 stem as well as a long straight neck and the selected head. On Figure 2c a modular neck is fixated and measured by the CMM and the resulting data is exported as an IGES file. The most important factor when measuring the modular necks was the accuracy for the top free area (Fig 2c) in relevance to the fixation level, since their in-between angle and relative position defines the usage of each neck (ante/retro, varus/valgus). Finally, on Figure 2d the CAD model – as an assembly – of the implant is presented.
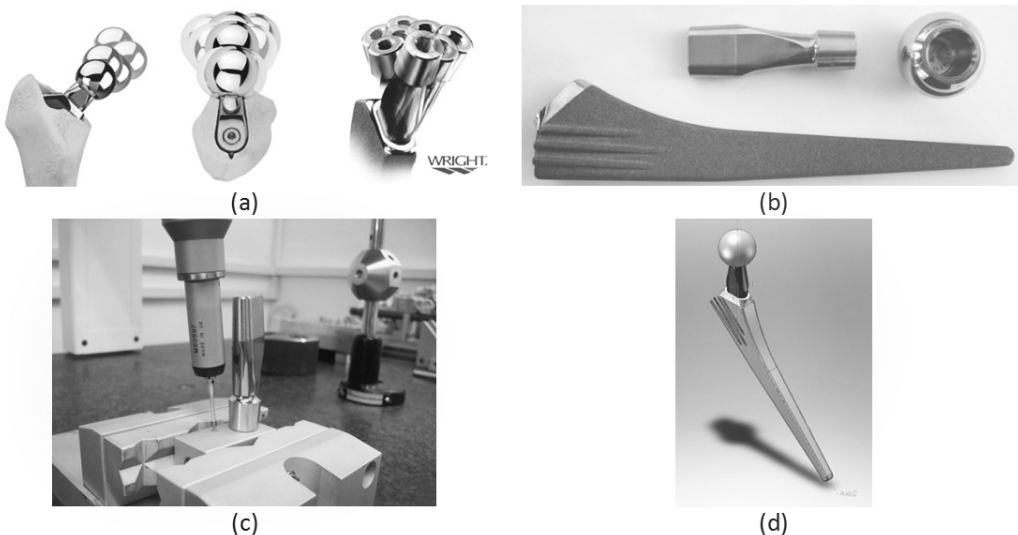

Figure 2. CMM Measurements and final CAD Model: a) Profemur System – Neck Modularity, b) Profemur-E Hip Implant, c) Coordinate Measurement Machine – Neck Measurements, d) CAD final implant geometry

2.3 Finite Element Model

Having the femur and the implant imported into the CAD software and according to the medical guidelines and the surgical procedure – for the specific implant type – provided by the manufacturer, the implant is positioned inside the bone volume.
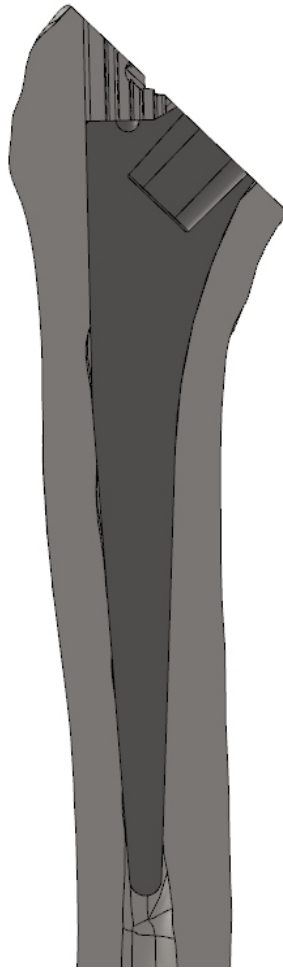
Figure 3. Section View of the CAD model, illustrating the achieved contact and fixation between femur and implant

Figure 3 demonstrates a section view of the CAD models of the bone and the stem in its final position. It is noted that in the model a satisfying degree of contact between the stem and the bone has been achieved (Iorio et al. 2008; Icavo et al. 2008). According the manufacturer notes, the head and the neck are fixated through a $12^o/14^o$ cone and the neck with the stem through a *tapered shaped oval slot*. The main stem is proximally in full contact with the bone volume and finally the stem tip is free, as required for a proper placement.

The transition from the CAD model to the Finite Element model was accomplished through the GUI of Ansys Workbench v.11 (ANSYS, Inc.), where the model is finally imported directly from SolidWorks. The F.E. Model consists of approximately 95.000 ten-node tetrahedra elements (Fig. 4).
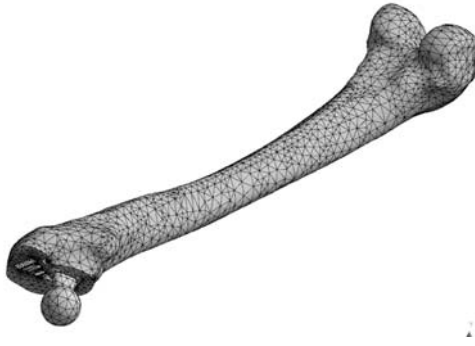
Figure 4. Full finite element model consisting of approximately 95.000 ten-node tetraedra elements.

2.4 Loading Scenario & Material Properties

For the finite element model, linear elastic isotropic material properties were assigned to all materials involved. The modulus of elasticity for the bone volume is E = 17000MPa and the Poisson ratio ν = 0.33 (Knauss, 1981). For the Profemur – E implants the corresponding values, according to the manufacturer, are:

- CoCrMo Head: E_{Head} = ~ 200 GPa and Poisson $ν_{Head}$ = 0.3

- CoCrMo Neck: E_{Neck} = ~ 240 GPa and Poisson $ν_{Neck}$ = 0.3

- Ti-Alloy Stem: E_{Stem} = ~ 110 GPa and Poisson $ν_{Stem}$ = 0.35

For the current study, one typical loading case was examined. Taking into account the bibliographic references, it was decided to investigate the one-legged stance phase of the gait cycle (Bergmann et al., 1993; Verdonshot and Huiskes, 1997). The following table (Table 1) summarizes the loads applied in the FE model. Figure 5 displays the boundary conditions - fully fixed - applied on the lower region of the femur and the two loads imposed on the upper part of the femur.

Figure 5. Boundary conditions of the finite element model: A) Lower region, fully fixed, B) Resulting muscle force, C) Femoral head loading.

Applied on	Magnitude (N)	Angle α (frontal plane)	Angle β (sagittal plane)
Femoral Head (Prosthetic Head)	2450	23º	6º
Greater Trochanter (*gluteus minimus*, *medius* and *maximus*)	1650	24º	15º

Table 1. Finite Element Model Loading – Stance Phase.

3. Results

It must be taken into account that all external loads were imported as nodal loads and the contact interfaces between the different volumes were treated as fully bonded by the solver. The above assumptions led to some stress and strain concentrations of numerical nature, although these values were omitted during the result evaluation. The finite element analysis was performed using the default (*program controlled*) solver of ANSYS Workbench v.11. The project database consisted of six different finite element models according to the modular neck they involved. In the following table (Table 2) the models are summarized:

Modular Neck	Neck Code*	Modular Neck	Neck Code
Straight Short	1202	Straight Long	1204
Retroversion 8º Short	1232	Retroversion 8º Long	1234
Anteversion 15º Short	1242	Anteversion 15º Long	1244

Table 2. Model name designation, according to the commercial neck code number, * *according to product manual*

In order to quantify and compare the overall behavior of the six models due to the offset changes, their minimum and maximum values were normalized (Fig. 9) with respect to the values of the less complex geometry, the short and straight modular neck (1202). This was achieved using the following equation:

$$Value_{norm} = \left(\frac{Value_{current} - Value_{reference}}{Value_{reference}} \right)$$ (1)

where $Value_{norm}$ is the normalized difference, $Value_{current}$ is the value under investigation and $Value_{reference}$ is the corresponding values of the 1202 model. This was performed for the equivalent von Mises stress of the 28mm prosthetic femoral head, the modular neck, the stem and finally for the equivalent von Mises strains in the bone volume respectively (Fig. 6). It derives that, the equivalent von Mises strains of the femoral head (CoCrMo) are dropping w.r.t. to our reference model, with the exception of the 1242 case where an increase was noted (Fig. 6a). Based on this, the femoral head was not under thorough investigation for the current study. But upon the comparison of the modular neck stresses, a significant increase was recorded for all cases examined (Fig. 6b). It is worth mentioning that the worst case was found for the short retroverted neck 1232 and with the short anterverted 1242 following. As far as the stem is concerned (Fig. 6c), the long retroverted neck 1234 produced the higher values w.r.t. to the short straight. Finally, the maximum and minimum values for the femur strains were compared. Again all cases revealed values significantly higher than the 1202 model, especially for short retrovetred 1232 and long anteverted 1244.
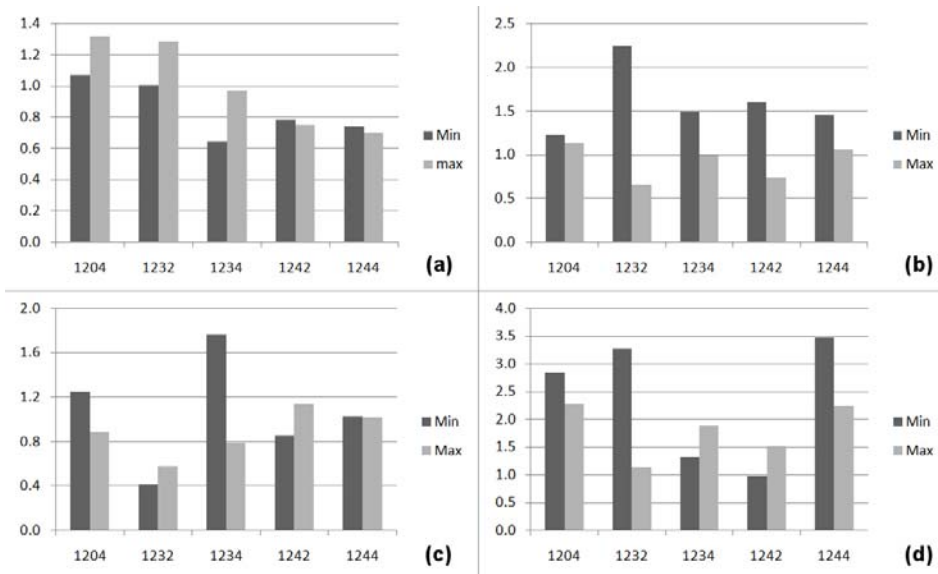

Figure 6. Variation of minimum and maximum values w.r.t. the Short & Straight Neck (1202):
a) 28mm normal head (Eq. V. M. Stress), b) modular necks (Eq. V. M. Stress),
c) Ti-Alloy stem (Eq. V. M. Stress), d) Femur volume (Eq. V. M. Strain)

In more details, in Figure 7 the developed equivalent von Mises stress fields on the 6 modular necks from two points of view, according to the bone orientation and position in the global coordinate system, are displayed: a) anterior view and b) posterior view. High stress concentrations near the contact regions with the femoral head are illustrated in all cases due to the contact conditions applied. Almost in all cases – with the exception of 1204 – two regions with higher values appear on the upper and lower rim of the head cone (*12/14 conical assembly of Morse type with the prosthetic head*). On the contrary, the lower region of the neck, namely the cone-like geometry that consolidates with the stem, did not reveal any peak values with the exception of neck 1232, where a small area had significant drop in values, but without causing any loading problems in the assembly. It was also noted, that the two long necks with ante and retroversion illustrated overall higher values, with the maximum found for the 1234 neck. We must also note an increase in stresses for the 1244 neck, in the narrow region, bellow the upper cone.
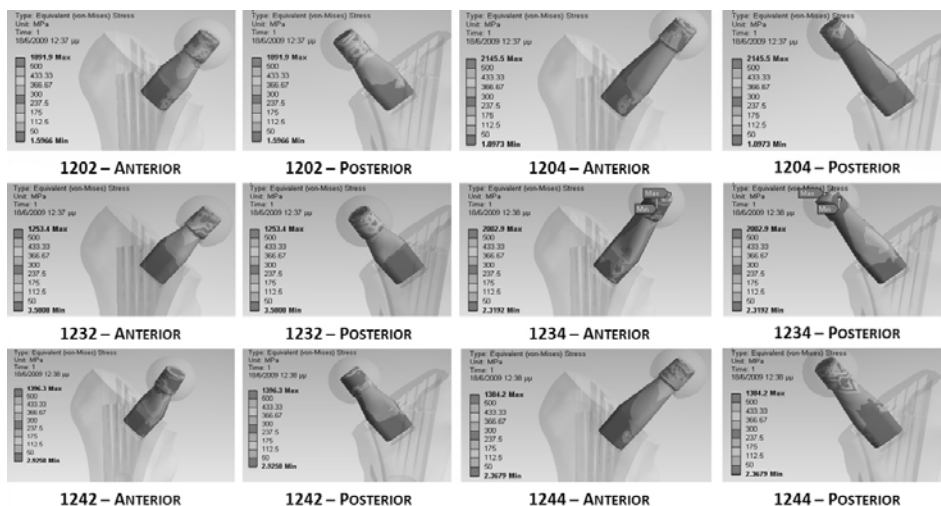
Figure 7. Modular Neck – Equivalent Von Mises Stress: Anteriorly & posteriorly

On Figure 8 the equivalent von Mises stress developed on the Ti-Alloy are illustrated. The three models 1232, 1234, 1244 (short & long retroverted & long anteverted), show significantly higher values and distributions, compared to the short necks, namely 10.32% - 18.78%. It was also revealed that the lower part of the anatomical fins had higher values, which is in compliance with the proximal fixation of the specific stem type.
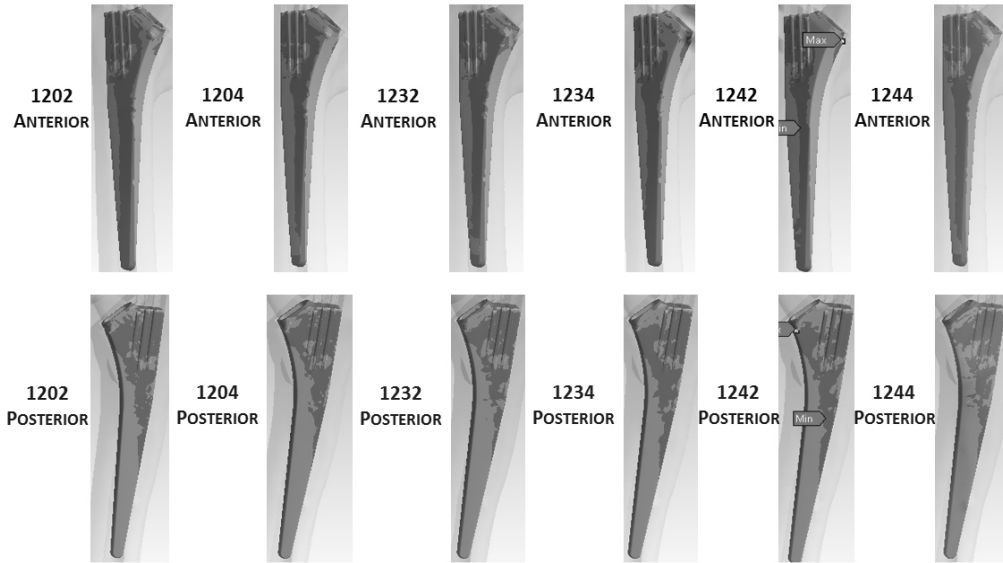
Figure 8. Ti Alloy Stem – Equivalent Von Mises Stress: Anteriorly & posteriorly

It must finally be noted that for all examined scenarios the stem and neck stresses *did not* exceed the material yield strength.

For Figure 9 the strain fields corresponding to each model were normalized with respect to Frost's bounds for bone absorption / remodeling (Frost 1992). According to Frost's theory, which is an extension of Wolff's law (Wolff 1982), the developed strains within the femur volume are responsible for bone remodeling activity. For values below the 300 μstrains limit, new bone is not developed normally and loss of bone occurs. For the middle zone bone conservation and strengthening occurs, tending to equal but not exceed the amount absorbed, the bone changes its architecture where and as needed to lower its strains, and healthy active growing of bone occurs. For higher values, peak strains lead to bone growth, which may or may not be positive.

As in the previous case (Fig. 6), the normalization concerned the individual nodal equivalent von Mises strain values and their distributions over the examined zone. In order to investigate whether the strain field in each case belonged to the aforementioned ranges or not, the following normalization was introduced:

$$\varepsilon_{norm,i} = \left(\frac{\varepsilon_{FEM,i} - \varepsilon_{Frost,lowerbound}}{\varepsilon_{Frost,upperbound} - \varepsilon_{Frost,lowerbound}} \right) \tag{2}$$

where $\varepsilon_{norm,i}$ is the normalized strain value of the $i-$model, $\varepsilon_{FEM,i}$ is the individual strain of each node / model estimated from the Finite Element Analysis, while $\varepsilon_{Frost,lowerbound}$ and $\varepsilon_{Frost,upperbound}$ are the lower and the upper bound for bone remodeling; it was set to 300 and 3000 μstrains, respectively. The estimated normalized values were finally allocated in three major classes, namely [0,300), [300,3000], (3000,max].
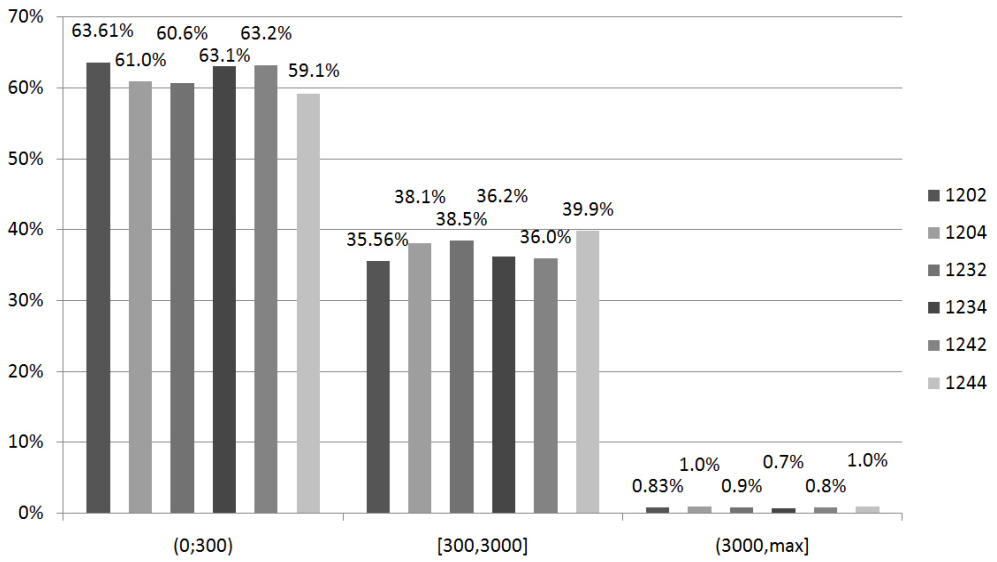
Figure 9. Equivalent von Mises µstrains with respect to Frost's Law for Bone Loss and Remodeling.
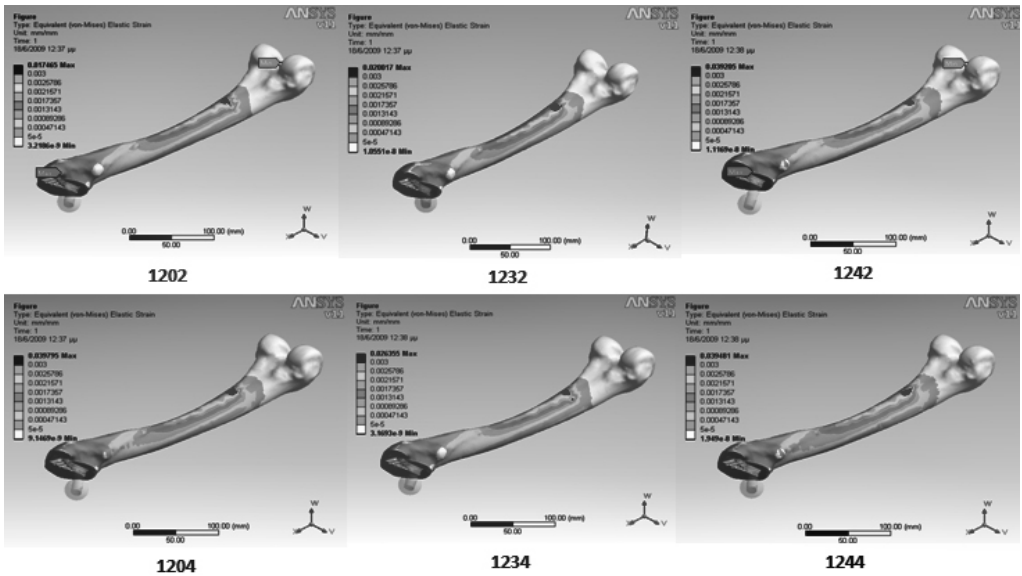

Figure 10. Distribution of the strain fields, with respect to Frost's law for bone absorption / remodeling for the six models, isometric view.

Furthermore the developed equivalent von Mises strain distributions on the femur volume, with respect to the upper and lower remodeling limits, are illustrated (Fig. 10). The white color denotes the regions with strains bellow the 300 µstrains limit, where no new bone is developed. We remind that the distal lower part is bellow this limit due to the fixation. With black color are the areas with strains above the 3000 µstrains limit. With significantly different distributions and values for the six models – ranging from 5% to 26% –it was noted that the lesser trochanter

had low strain values for the short necks. This correlates with possible bone loss in the future that may compromise implant stability in the long term.

By further examination of the results and taking into account the loading conditions of the model, the different offset – as introduced by the modular necks – produces different distributions. The validation of this behavior was one of the main goals for the current study and will provide useful information for the ongoing research.
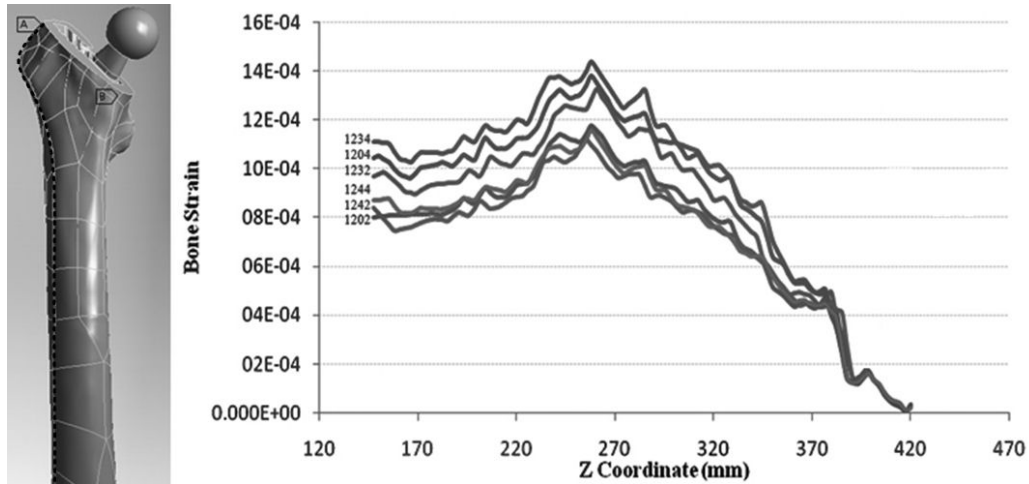
Figure 11. Equivalent von Mises μstrains along Z Axis – Profile line along the femur length including the greater trochanter, lateral side.

In order to isolate and clearly illustrate the effects of the six modular necks imposed on the strains of the femur, two profile lines were chosen and their node values were recorded. The first was on the lateral side of the femur, running along the greater trochanter. The 8°, long anteverted neck (1234) displayed the higher values approximately 30%. For z= 270 the maximum value is located and corresponded to the distal stem tip. The overall behavior again indicated that changing from short to long neck, a significant increase in values occurred; an average value for the three pairs of 23.68% was recorded. It could be stated that through the z axis, along the line path, all six models display similar behavior. At the height of z = 390mm the six models converge to a minimum value of approximately 100 μstrains, reaching the osteotomy plane.
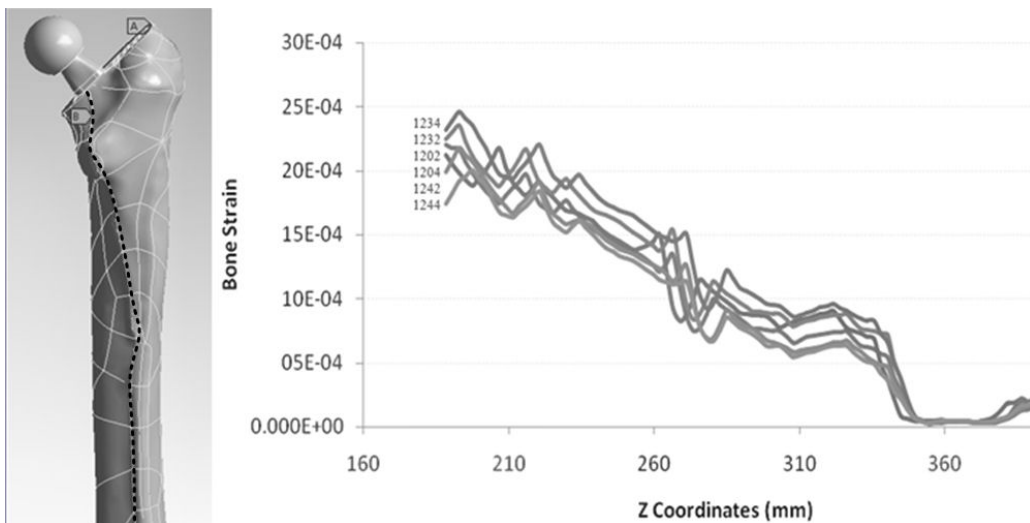
Figure 12. Equivalent von Mises μstrains along Z Axis – Profile line including the minor trochanter and linea aspera, medial side.

The other profile line started at the osteotomy level, over the lesser trochanter and along linea aspera, an anatomical element of the femur geometry. The same behavior as previously is illustrated in Figure 12. A more uniform distribution is displayed here among the six models. The value fluctuation reached approximately 12% – 18%.

The 1234 neck had the higher values. Again approximately for z = 270mm a significant drop was recorded in strains at the stem tip region. For the lesser trochanter – at z = 350mm – a drop was also recorded representing lower strain region shown in Figure 10. Finally, it must be noted that convergence occurred again for z = 350 mm to z = 380mm with values near zero at the osteotomy plane. Comparing the maximum values of the two graphs, it is clearly visible that the line crossing the minor trochanter suffers from much higher strain values (~ *45 – 65 % increase*) as anticipated due to the loading applied, a phenomenon which also appears upon clinical investigations among patients (Weinans et al. 1991).

4. Discussion and Conclusions

The aim of this study was to investigate the influence of the variable neck lengths used with commercial hip implant systems in THA operations. As stated (Bono J. 2001), the specific neck design provides extensive flexibility even intraoperatively but the use of several different materials for the implant parts and the implementation of additional interfaces between the collaborating parts increase the factors that must be evaluated and examined. In order to clearly isolate the influence of the neck modularity some presumptions had to be taken into account.

Extensive bibliographic research (Bergman et al. 1993; Stolk et al. 2001;) has also yet to reveal a clarified description and validation of the changes in the muscle forces involved, when modular components are used. This is also the case when different modular necks are introduced into the mathematical models. For the current study it was decided to maintain the same force values for all cases (Verdonschot et al. 1997). The material properties used in the finite element analysis must also be taken into consideration, since the bone was assigned linear elastic isotropic properties (Knauss, 1981), which does not correspond to the actual material.

The numerical analysis revealed that the stress and strain distributions within the implants and the femur were subject to the offset changes and the alteration of the modular necks. The quantitative data analysis performed, detected a significant amount of nodes suffering from bone loss (Abdul-Kadir et al. 2008), such as the in the lesser trochanter. The finite element analysis also revealed that changing from short neck to long necks, the strains in specific lateral areas in the femur volume increase (Aamodt et al., 1997) that may lead to positive bone growth and strengthening. More specifically three necks were under higher values, namely short and long retroverted (1232 & 1234) and long anteverted (1244) which will require further examination, in comparison to clinical data. Finally, the stress values on the modular neck did not overcome the yield strength of the commercial CoCrMo used, but areas with high concentrations exist, leading to further analysis along with the implementation of nonlinear contact analysis for the interfaces.

In conclusion, it is undisputed that the use of modular implants in the area of Hip Arthroplasty is of great importance: they promise to provide flexibility for the surgeons and long-term stability for the patients. Several aspects are still under thorough investigation and research by the authors with respect to the modularity of the commercial designs.

Acknowlegments

References

Aamodt A, Lund-Larsen J, Eine J, Andersen E, Benum P, Husby O (1997). In vivo measurements show tensile axial strain in the proximal lateral aspect of the human femur. *Journal of Orthopaedic Research*, 15, 927 – 931.

Abdul-Kadir M, Hansen U, Klabunde R, Lucas D, Amis A (2008). Finite element modelling of primary hip stem stability: The effect of interference fit. *Journal of Biomechanics*, 41, 587 – 594.

Bergmann G, Graichen F, Rohlman A (1993). Hip joint loading during walking and running, measured in two patients, *Journal of Biomechanics*, 26, 969-90.

Bono J (2001). S-ROM modular total hip replacement. *Operative Techniques in Orthopaedics*, 11, 279-287.

Brinker M, Rosenberg A, Kull L, Galante J (1994). Primary Total Hip Arthroplasty Using Noncemented Porous-coated Femoral Components in Patients With Osteonecrosis of the Femoral Head, *The Journal of Arthroplasty*, 9, 457 – 468.

Charnley J, 1972. The long-term results of low-friction arthroplasty of the hip performed as a primary intervention. *The Journal of Bone and Joint Surgery*, 54, 62 – 76.

Chu Cheng-Mien, Wang Shyu-Jye, Lin Leou-Chyr (2001). Dissociation of modular total hip arthroplasty at the femoral head–neck interface after loosening of the acetabular shell following hip dislocation, *The Journal of Arthroplasty*, 16, 806-809.

Completo A, Fonseca F, Simões J (2007). Experimental validation of intact and implanted distal femur finite element models. *Journal of Biomechanics*. 40, 2467-2476.

Della Valle A, Padgett D, Salvati E (2005). Preoperative Planning for Primary Total Hip. *Journal* of the American Academy of Orthopaedic Surgeons, 13, 455 – 462.

Dostal W, Andrews J (1981). A three-dimensional biomechanical model of hip musculature. *Journal of Biomechanics*, 14, 803 – 812.

Incavo S, Beynnon B, Coughlin K (2008). Total Hip Arthroplasty with the Secur-Fit and Secur-Fit Plus Femoral Stem Design: A Brief Follow-Up Report at 5 to 10 Years, *The Journal of Arthroplasty*, 23, 5, 670-676.

Iorio R, Healy W, Presutti A (2008). A Prospective Outcomes Analysis of Femoral Component Fixation in Revision Total Hip Arthroplasty, *The Journal of Arthroplasty,* 23, 5 662-669.

Knauss P (1981). Material properties and strength behavior of the compact bone tissue at the coxal human-femur. *Biomedical Techniques* 26, 311-315.

Min B, Song K, Bae K, Cho C, Lee K, Kim H (2008). Second-Generation Cementless Total Hip Arthroplasty in Patients With Osteonecrosis of the Femoral Head, *The Journal of Arthroplasty*, 23, *902-910*.

Rietbergen B, Huiskes R, Weinans H, Scimner D , Turner M, Galante J (1993). The mechanism of bone remodeling and resorption around press-fitted tha stems. *Journal of Biomechanics*, 36, 369-382.

Sariali E, Mouttet A, Pasquier G, Durante E (2009). Three-Dimensional Hip Anatomy in Osteoarthritis: Analysis of the Femoral Offset, *The Journal of Arthroplasty*, *24, 990-997*.

Sariali E, Veysi V, Stewart T (2008). (i) Biomechanics of the human hip e consequences for total hip replacement, *Current Orthopaedics*, 22, 371-375.

Sporer Scott M, DellaValle Craig, Jacobs Joshua, Wimmer Markus (2006). A Case of Disassociation of a Modular Femoral Neck Trunion After Total Hip Arthroplasty, *The Journal of Arthroplasty*, 21, 918-921.

Stolk, J., Verdonschot, N., Huiskes, R., 2001. Hip-joint and abductor-muscle forces adequately represent in vivo loading of a cemented total hip reconstruction. *Journal of Biomechanics*, 34, 917-926.

Verdonschot N, Huiskes R (1997). Acrylic cement creeps but does not allow much subsidence of femoral stems, *JBJS*, 79, 665 – 669.

Weinans H, Huiskes R, Verdonschot N, Rietbergen B (1991). The effect of adaptive bone remodeling threshold levels on resorption around noncemented hip stems, *BED*, 20, 303 – 306.

Werner A, Lechniak Z, Skalski K, Kedzior K (2000). Design and manufacture of anatomical hip joint endoprostheses using CAD/CAM systems, *J Mat Proces Tech*, 107, 181-186.

Wolff J (1982). The Law of Bone Remodeling, Berlin Heidelberg New York, Springer (*translated in 1986)*

List of Figures

List of Tables